Applied Catalysis B: Environmental 96 (2010) 290–298

Contents lists available at ScienceDirect

Applied Catalysis B: Environmental

journal homepage: www.elsevier.com/locate/apcatb

Degradation of microcystin-LR using sulfate radicals generated through photolysis, thermolysis and e⁻ transfer mechanisms

Maria G. Antoniou [a], Armah A. de la Cruz [b], Dionysios D. Dionysiou [a,*]

[a] Department of Civil and Environmental Engineering, University of Cincinnati, Cincinnati, OH 452211-0071, USA
[b] Office of Research and Development, U.S. Environmental Protection Agency, Cincinnati, OH 45268-1314, USA

ARTICLE INFO

Article history:
Received 21 August 2009
Received in revised form 9 November 2009
Accepted 5 February 2010
Available online 19 February 2010

Keywords:
Cyanotoxins
e⁻ transfer mechanisms
Microcystin-LR
Fenton Reagent
Hydrogen peroxide
Oxidants
Persulfate
Peroxymonosulfate
Photolysis
Sulfate radicals
Thermolysis

ABSTRACT

This study explores the potential use of sulfate radical-based advanced oxidation technologies (SR-AOTs) for the degradation of the naturally occurring hepatotoxin, microcystin-LR (MC-LR). The generation of sulfate radicals was achieved by activation of the oxidants persulfate (PS) and peroxymonosulfate (PMS) through electrophilic transition metal cations (Ag^+ and Co^{2+}, respectively), radiation (UV $300 < \lambda < 400$ nm) and/or heat ($T = 30\,^{\circ}C$). These systems were compared to more frequently used AOTs systems in industrial applications; the Fenton Reagent (FR) and hydrogen peroxide coupled with heat and radiation. Even though $SO_4^{\bullet -}$ has similar redox potential to hydroxyl radical ($HO^{\bullet}$), to the best of our knowledge, SR-AOTs have not been tested for the degradation of cyanotoxins. In this study, PMS was activated very efficiently with Co^{2+} at neutral pH and increasing catalyst concentration resulted in dramatic increase of the initial rates of degradation that reached a plateau for $C_{Co(II)} \geq 1$ mg. Based on the optimum pH conditions for each system, the efficiency order is $Co^{2+}/PMS > Fe^{2+}/H_2O_2 \gg Ag^+/PS$, which we believe is associated with the energy of the lower unoccupied molecular orbital of the oxidants. When UV ($300 < \lambda < 400$ nm) radiation was used, the PS system was more efficient than PMS and H_2O_2 at all different oxidant concentrations.

Since, the UV lamps used in the study emit light at a range of wavelengths ($300 < \lambda < 400$ nm), the activation of the oxidants is believed to be caused by the emission spectra and not just $\lambda_{max} = 365$ nm. At acidic conditions, the PS/UV ($300 < \lambda < 400$ nm)/pH 3 and PMS/UV/pH 3 systems were most efficient and required the least amount of energy to reduce the toxin concentration by one order of magnitude. When thermal activation was used, PMS yielded the highest degradation efficiency (~77%) compared to 52% for the PS and less then 2.5% for H_2O_2.

1. Introduction

Cyanotoxins pose a significant health hazard to humans and wildlife [1]. Their increasing appearance in water resources is causing environmental (pollution), social (water supply restriction to millions of people) and economical (clean-up plans are in the billion dollar range) problems [1,2]. These toxic compounds are produced by approximately a third of cyanobacteria genera (50 out of 150 recorded) and are excreted to aquatic environments through cell metabolic reactions or released after cell rupture [3]. The appearance of cyanotoxins becomes more profound during the eutrophication of water bodies, where the likelihood for growth of hazardous cyanobacteria genera considerably increases and results in the formation of cyanobacterial harmful algal blooms (Cyano-HABs). Since a single strain of cyanobacteria can produce upto 12 different types of toxins, exposure to contaminated water can affect mammalian health in a variety of ways including irritation of the skin and vital organs (dermatotoxins and irritant toxins), cell damage (cytotoxins), liver failure (hepatotoxins), or permanent effects on the nervous system (neurotoxins) [4–10]. One cyanotoxin, microcystin-LR (MC-LR), a hepatotoxin and a tumor promoter from the group of microcystins, has particularly captured the scientific interest and created concerns to environmental and human health authorities because of its frequency of appearance and persistence in natural waters [1,11–13].

MC-LR exhibits higher lethality than the venom of dangerous snakes such as cobra ($LD_{50,MC\text{-}LR} = 50\,\mu g/kg$ vs. $LD_{50,cobra} = 500\,\mu g/kg$) and since regulations for all cyanotoxins are still pending [14], a variety of technologies is currently been tested for their treatment [1,11]. The inability of conventional water treatment processes to decompose recalcitrant contaminants has instigated the utilization of emerging chemical oxidation water treatment processes such as advanced oxidation technologies (AOTs). AOTs utilize oxidants, catalysts and/or radiation, or

* Corresponding author. Tel.: +1 513 556 0724; fax: +1 513 556 2599.
E-mail address: dionysios.d.dionysiou@uc.edu (D.D. Dionysiou).

0926-3373/$ – see front matter © 2010 Elsevier B.V. All rights reserved.
doi:10.1016/j.apcatb.2010.02.013

their combination, for the generation of highly active, oxidizing species such as HO• and other radicals. The investigation of the potential use of AOTs for the treatment of drinking water and wastewater has been attractive to scientists and engineers, since the radical species formed imitate naturally occurring oxidation processes (i.e., biological treatment) but at accelerated rates [15].

Radical species can be formed in homogeneous systems *via* electron transfer by transition metal activation of the oxidants [16,17], *via* photolysis of oxidants [18], *via* thermolysis of oxidants [19–21], and sonolysis [22,23] or in heterogeneous systems (i.e., TiO_2 photocatalysis) [24–30]. The most commonly used homogeneous system in the water treatment industry is the coupling of iron (Fe^{2+}) with hydrogen peroxide (H_2O_2) for the formation of HO• radicals, also known as the Fenton Reagent (FR) [31]. However, FR has major limitations including narrow functional pH in the acidic range, iron precipitation, slow kinetics of ferrous ion regeneration and the requirement of high concentrations of iron (stoichiometric ratios) for the system to be efficient [17]. In this study, modified oxidation reagents based on the FR chemistry were evaluated for the degradation of cyanotoxins [16–18,32–34]. Similarly with FR, these systems incorporate a transition metal (cobalt or silver) with an oxidant (peroxymonosulfate, PMS or persulfate, PS) for the generation of highly oxidizing species (sulfate radicals, $SO_4^{\bullet-}$). Previous studies in our group [17,18] have revealed that the Co^{2+}/PMS system could overcome some of the major constrains of FR. In addition, $SO_4^{\bullet-}$ radicals have higher standard redox potentials than HO• radicals for the abduction of electrons, 2.5–3.1 V [35,36] and 1.89–2.72 V [37], respectively, yet there are limited studies on sulfate radical-based AOTs for the degradation of recalcitrant organic contaminants [33].

Interest in the chemistry of sulfur-oxygen radicals $SO_n^{\bullet-}$ (n = 3, 4, 5) was intensified after their involvement in the conversion of $SO_{2(g)}$ to acid rain (H_2SO_4) was understood [38]. Many studies have been conducted to examine the pathways that result to $SO_n^{\bullet-}$ formation, their redox potentials and oxidation mechanisms as well as their preferable mechanistic oxidation routes [36]. The strongest oxidant is the $SO_4^{\bullet-}$ (sulfate radical), followed by $SO_5^{\bullet-}$ (peroxymonosulfate radical, redox potential 1.1 V, at pH 7) and $SO_3^{\bullet-}$ (sulfite radical, redox potential 0.63 V, at pH 7). All these radicals give weak absorption in the UV–vis spectra ($\lambda_{SO_4} = 450$ nm, $\varepsilon_{SO_4} = 1100\ M^{-1}\ cm^{-1}$; $\lambda_{SO_5} = 260$ nm, $\varepsilon_{SO_5} = 1030\ M^{-1}\ cm^{-1}$; $\lambda_{SO_3} = 250$ nm, $\varepsilon_{SO_3} = 1380\ M^{-1}\ cm^{-1}$), but since the sulfate radicals have short lifetimes (30–40 μs), [39] they can only be detected by transient absorbance spectroscopy and amplification of the signal [39]. $SO_5^{\bullet-}$ and $SO_3^{\bullet-}$ are strongly selective in their reactions [40] and $SO_3^{\bullet-}$ is a poor reductant that is not oxidized by e^- transfer processes but rather *via* O^- transfer [36]. On the other hand, $SO_4^{\bullet-}$ radicals are among the strongest oxidants known, much stronger than oxidants commonly used in industry, such as permanganate (E = 1.70 V) [41] and hypochlorous acid (E = 1.49 V) [42]. Among the known oxidants used in water treatment applications, only HO• (hydroxyl radicals) have redox potentials (E = 2.72 V) close to the $SO_4^{\bullet-}$ [37].

According to a study by Neta et al. [36], owing to their selectivity, sulfate radicals are more efficient oxidants for organic compounds with unsaturated bond and aromatic constituents than the hydroxyl radicals [43]. So far, PS and PMS (the oxidants that primarily generate $SO_4^{\bullet-}$) have been used for the treatment of wastewater contaminated with industrial toxins [18,33,44–47] in combination with other AOTs such as TiO_2 photocatalysis to enhance degradation rates [48], as bleaching agents in the paper pulp industry to avoid DBPs formation [49,50], in soil remediation [19,20,45], in TOC analyzers [51], for measuring UV-C fluxes [52] and in chemical reactions such as asymmetric epoxidations [53]. More recent studies have expanded the use of SR-AOTs in chemical and microbial decontamination of swimming pool water [34].

This study investigates different methods for the formation of sulfate radicals as potential emergency response technologies to cyanobacterial toxins contamination. To the best of our knowledge, this is the first study of its kind on the degradation of cyanotoxins with sulfate radicals. The radicals were generated from the activation of the oxidants peroxymonosulfate and persulfate via: (i) electron transfer from transition metals, (ii) UV ($300 < \lambda < 400$ nm) and (iii) thermal decomposition. These activation processes can be selective towards one type of radicals, $SO_4^{\bullet-}$ or HO• (radiation and heat) or can resolve in a mixture of radicals $SO_4^{\bullet-}$and HO• (transition metals). The effects of operational parameters on the MC-LR degradation (oxidant concentration, catalyst concentration and pH) were observed and SR-AOTs were compared with FR and H_2O_2 systems.

2. Experimental

2.1. Safety

Due to the hazardous nature of the toxin, all experiments were conducted in an Advance SterilchemGARD III Class II Biological Safety Cabinet (The Baker Company, Sanford, ME) with full exhaust.

2.2. Materials and methods

A 482 mg/L stock solution of MC-LR was prepared by dissolving 0.5 mg of solid MC-LR (CalBiochem, 96.4% by HPLC; FW = 995.2 g/mol) with 1 mL of autoclaved Milli-Q® Synthesis A10 water (MQ-H_2O, Millipore Corp., Billerica, MA, USA; resistivity = 18.2 MΩ; conductivity = 0.05 μS/cm). Different toxin concentrations (1–10 μM) were achieved by spiking specific aliquots (range of μL) of the 482 mg/L standard solution in pre-adjusted pH solutions, or MQ-H_2O water.

The catalysts for the activation of the oxidants were transition metals in their lowest oxidation states. $CoCl_2{\cdot}6H_2O$ (Aldrich), Ag_2SO_4 (Fisher), and $FeSO_4{\cdot}7H_2O$ (Fisher) were used as the sources of cobalt (II), silver (I) and iron (II), respectively. Stock solutions of the metal salts were prepared with concentration of 2.945 g M^{n+}/L. The stock solutions were further diluted 1000 and 10,000 times to give new stock solutions used in the experiments. In the case of iron (II), the 2.945 g/L initial stock solution was prepared in MQ-H_2O acidified with 5 N H_2SO_4 (pH_{final} 1.7).

The oxidants used in this study were potassium peroxymonosulfate (PMS, HSO_5^-), potassium persulfate (PS, $K_2S_2O_8$, Fisher) and hydrogen peroxide (H_2O_2, 50% solution, Fisher). OXONE® (95%, Dupont) is the commercial name of the triple-salt $2KHSO_5{\cdot}KHSO_4.K_2SO_4$ that releases PMS during dissociation. Stock solutions of 40 and 4 mM of oxidants were freshly prepared in MQ-H_2O.

The quantification of the toxin was performed with an Agilent 1100 Series quaternary LC (liquid chromatograph) equipped with a photodiode array detector (PDA) set at 238 nm. A C_{18} Discovery HS (Supelco) column (4.6 mm × 150 mm, 3 μm particle size) was utilized as a stationary phase, while the mobile phase was a mixture of 0.05% (v/v) trifluoroacetic acid (TFA) in acetonitrile solution and 0.05% (v/v) TFA in MQ-H_2O in 40:60 ratio. The analysis was conducted under isocratic conditions and MC-LR eluted at about 5.4 min. The flow rate was set at 1 mL/min and the injection volume was 50 μL. The temperature of the column was set at 40 °C. Details on the analytical methods (isocratic and gradient) are reported elsewhere [25,28,29]. The UV–vis spectra of MC-LR and the oxidants were obtained using a single beam Spectramax M2 spectrophotometer (Molecular Devices Corp., Sunnyvale, CA, USA).

2.3. Experimental setup

The experiments were conducted using 10 mL solutions in 40 mL dark borosilicate glass vials at ambient temperature (T_{ROOM} = 25 °C). Samples (100 μL) were taken at specific time intervals and then quenched with 100 μL of methanol (Aldrich). For experiments where oxidants were activated with irradiation, 10 mL of MC-LR solution (of predetermined concentration and pH) was placed in sealed round pyrex reactor vessels (diameter = 10 cm) and illuminated from the top with two long wave 15 W UV lamps (Cole-Parmer, 300 nm < λ < 400 nm, with λ_{max} = 365 nm) [54]. The lamps used in this study emit light in the UVA (320 nm < λ < 400 nm) and part of the UVB range (280 nm < λ < 320 nm). For this reason, the lamps instead of UV (300 nm < λ < 400 nm) will be called UVA* for simplicity. A fan was used to cool the reactor (T = 25.5 ± 0.5 °C). The intensity of the lamps was also measured with potassium ferrioxalate actinometry [55]. The quantum yield of ferrous production at λ = 365 nm is φ_λ = 1.27 ± 0.02 [56]. The average light intensity from the lamps was 5.58 ± 0.94 × 10^{-5} einstein/s. Based on the Planck–Einstein equation $E = hc/\lambda$, where h is Planck constant, the quantum energy that is contained by a photon at wavelength λ = 365 nm is E_{365} = 5.44 × 10^{-19} J/photon. Multiplication of E_{365} with the Avogadro's Number transforms the units in E_{365} = 327,554 J/einstein [57]. The photon flux (P_{365}) of the reactor is obtained by multiplying the estimated average irradiation with the quantum energy E_{365} and is equal to 18.28 W. Since the lamps used in the study are emitting at a range of wavelengths (300 nm < λ < 400 nm), which may assist in the activation of the oxidants, the equivalent values at λ = 313 nm were also estimated. For φ_λ = 1.24 ± 0.02 [56], the average light intensity was 5.71 ± 0.95 × 10^{-5} einstein/s and photon flux (P_{313}) = 21.82 W.

For the thermal activation of the oxidants, 3 mL toxin solution was placed in a quartz cuvette (λ = 1 cm) in a UV–vis spectrophotometer by *Molecular Devices*, with a controlled thermostat for t = 3.5 h. The UV–vis spectra of the oxidants, toxin and their mixtures were taken at T = 25 °C, while the thermolysis was performed at T = 30 °C.

2.4. Statistical and structural analysis

GraphPad Prism 4 software was utilized for the statistical analysis of the experimental data. For the comparison between two values (initial rates), t-test was used. The null hypothesis tested was that values are not different (H_o: $\mu_1 = \mu_2$) while the alternative was the values are different (H_a: $\mu_1 \neq \mu_2$). All the tests were two sided for α = 0.05 (α being the null hypothesis rejection probability). The degradation curves were fitted with the *first order* kinetic model.

3. Results and discussion

3.1. Activation of oxidants with catalyst

Previous results in our group from the degradation of recalcitrant organic contaminants with SR-AOTs [16–18,32–34,44–47] propelled our interest to also test the efficiency of such processes for the treatment of cyanotoxins and specifically in this study, MC-LR. PMS is activated by electron transfer mechanisms from cobalt cations for the generation of mainly sulfate radicals (Eqs. (1) and (3)). Hydroxyl and peroxymonosulfate radicals are also generated (Eqs. (4) and (2), respectively) [16]. The biggest advantage of this system is that the reverse electron transfer from Co^{3+} to Co^{2+} is thermodynamically feasible (0.82 V) [16]. The regeneration of the catalyst makes the system catalytic and the reaction can proceed cyclically until PMS is completely consumed given enough reaction time (Eq. (2)). Moreover, the catalyst-mediated decomposition of

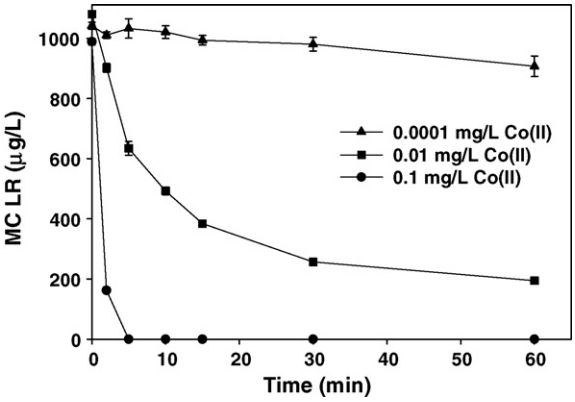

Fig. 1. Degradation of MC-LR with the Co(II)/PMS system at different Co(II) concentrations [$C_{MC\text{-}LR}$ = 1.0 μM; [PMS]/[MC-LR] molar ratio = 10/1; pH_o 6.24].

the oxidant PMS, depending upon the transition metal used as a catalyst and its oxidation state, can proceed with the formation of sulfate or hydroxyl radicals [58,59]. For example, Fe^{2+} and Ti^{3+} result in the formation of $SO_4^{\bullet-}$ and HO• radicals, however Cu^{2+} selectivity forms HO• [38,60]. At strong acidic conditions, hydroxyl radicals can react with sulfate groups and oxidize them to sulfate radicals or their corresponding hydroxylated form (Eq. (5)). No pK_a constant has been assigned for the protonation of sulfate radicals [36]. The peroxymonosulfate radicals can also react with each other to produce sulfate radicals and oxygen (Eq. (6)) [16,60,39,61,62].

$$Co^{2+} + HOOSO_3^- \rightarrow Co^{3+} + SO_4^{\bullet-} + HO^- \quad (1)$$

$$Co^{3+} + HOOSO_3^- \rightarrow Co^{2+} + {}^{\bullet}OOSO_3^- + H^+ \quad (2)$$

$$HOOSO_3^- + e^- \rightarrow SO_4^{\bullet-} + HO^- \quad (3)$$

$$HOOSO_3^- + e^- \rightarrow SO_4^{2-} + HO^{\bullet} \quad (4)$$

$$HO^{\bullet} + SO_4^{2-}(HSO_4^-) \xrightarrow{k=1.18\times10^6\,M^{-1}\,s^{-1}} SO_4^{\bullet-}(HSO_4^{\bullet}) + HO^- \quad (5)$$

$$2HSO_5^{\bullet} \leftrightarrow HO_3SOOOOSO_3H \rightarrow \{SO_4^{\bullet-}OOSO_4^{\bullet-}\} + 2H^+ \rightarrow 2SO_4^{\bullet-} + O_2 + 2H^+ \quad (6)$$

Control experiments were conducted in the absence of oxidant and/or catalyst. Under our experimental conditions no losses of the toxin were found because of volatilization or dark oxidant activation (Fig. 4 for controls). Degradation was only observed in the presence of catalyst and oxidant (for these experimental conditions) (Fig. 1). The optimum catalyst concentration for the efficient degradation of MC-LR was initially investigated. At increased catalyst loading from 0.0001 to 0.1 mg/L Co^{2+}, the initial rate of degradation increased drastically, as shown in Fig. 2. When 1.0 mg/L cobalt was used (results not shown) the activation was so fast that at treatment time 2 min, the peak of MC-LR completely disappeared from the LC-chromatogram. For catalyst 1 mg/L and above, the initial rates reach a plateau which means that low concentrations of catalyst (even lower from what was previously mentioned in the literature [18]) are sufficient for the system to be efficient.

One concern about the application of sulfate radicals into natural water is their ability to oxidize Cl^- to chlorine radicals ($Cl^{\bullet}$) [36] that have lower redox potential than sulfate radicals and slow down the degradation rates. $Cl^{\bullet}$ can also react with organics and form chlorinated by products [33]. However, high concentrations of Cl^- are required for this to occur [33]. The Co^{2+} salt used as catalyst in this study was $CoCl_2{\cdot}6H_2O$ which can yield Cl^- in the matrix. However, studies performed on the identification of reaction intermediates

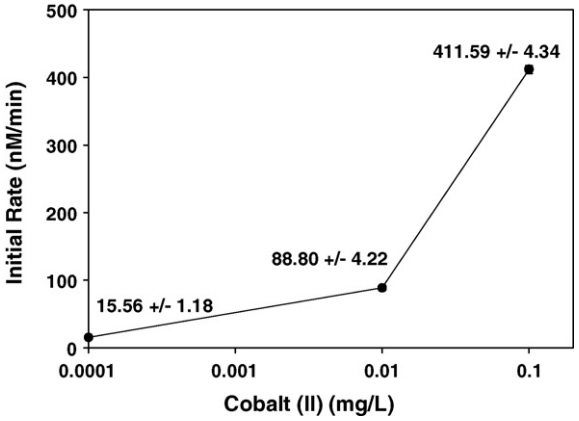

Fig. 2. Initial rates of MC-LR degradation with the Co^{2+}/PMS system at different Co(II) concentrations (*x* axis is in logarithmic scale) [$C_{MC\text{-}LR}$ = 1.0 μM; [PMS]/[MC-LR] molar ratio = 10/1; pH_o 6.24].

(results in an upcoming publication), did not show any chlorinated intermediates probably because of the low concentrations of the catalyst and therefore chloride was used. As far as slowing down of the kinetics, other studies have reported no difference in the degradation efficiencies of the Co/PMS when $CoSO_4$ and $CoCl_2$ are used as catalysts at higher concentration than in our study [49].

Another set of Me^{n+}/Ox that results in the formation of sulfate radicals (Eq. (7)) is silver with persulfate (Ag^+/PS) [17]. However, this system did not perform as well as the Co^{2+}/PMS system. After 4 h treatment of 1.01 μM MC-LR in the presence of 0.93 μM Ag^+ and molar ratio of [PS]/[MC-LR] = 10, no degradation was observed (Fig. 3). Studies where this system was utilized for the degradation of chlorophenols, at the same oxidant to contaminant molar ratio (10/1) and acidic pH, stoichiometric concentrations of Ag^+ (50 mg/L) were necessary in order to obtain sufficient degradation (~80%) [18]. In our studies, the silver concentration was within its solubility range (Ag_2SO_4 = 8.3 g/L) and no adjustment of the pH was performed to avoid changes in the chemistry of the free radicals in solution [37] and to allow comparison with the Co^{2+}/PMS system. Since Ag^+ has been used in the paper pulp industry to inhibit cellulose decomposition by quenching $SO_4^{\bullet-}$ (Eqs. (8) and (9)) [49,50], we believe, that under our experimental conditions, the increasing quenching rate of the $SO_4^{\bullet-}$ from Ag^+ compare to their generation rate reduces significantly the degradation of MC-LR. $SO_4^{\bullet-}$ radicals have comparable chances to react with MC-LR and Ag^+ since they were used in comparable concentrations and have the same second order reaction rate constants [$k_{Ag/SO_4} = 3.0 \times 10^9\ M^{-1}\ s^{-1}$, [49,50]; $k_{Ar/SO_4} = 3.0 \times 10^9\ M^{-1}\ s^{-1}$ (Ar, aromatic ring) [43])]. A similar quenching reaction can occur by Co^{2+}, however studies have shown that Ag^+ is a more efficient $SO_4^{\bullet-}$ scavenger Eq. (10) ($k_{Co/SO_4} = 2.0 \times 10^6\ M^{-1}\ s^{-1}$) [36,62]. To overcome this, high concentrations of Ag^+ are needed ($C_{Ag(I)}$ > 50 mg) [18,62,63].

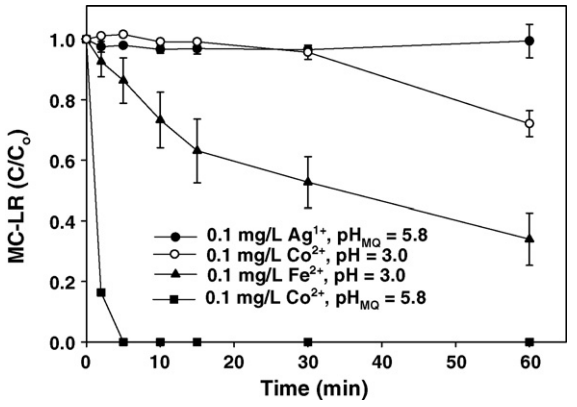

Fig. 3. Comparison of the efficiencies of the Co^{2+}/PMS, Ag^{1+}/PS, and Fe^{2+}/H_2O_2 systems for the degradation of MC-LR at similar experimental conditions [$C_{MC\text{-}LR}$ = 1.0 μM; [Ox]/[MC-LR] molar ratio = 10/1; Me^{n+} = 0.1 mg/L].

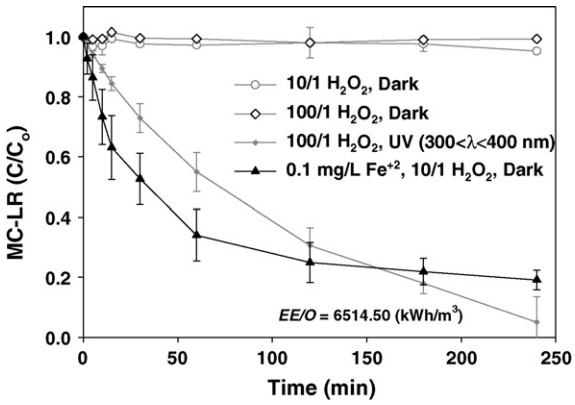

Fig. 4. Comparison of MC-LR with the H_2O_2/UV (300 < λ < 400 nm) system at neutral pH with the Fenton Reagent and control experiments [$C_{MC\text{-}LR}$ = 1.0 μM; [H_2O_2]/[MC-LR] molar ratio = 10 and 100].

$$Ag^+ + S_2O_8^{2-} \rightarrow Ag^{2+} + SO_4^{\bullet-} + SO_4^{2-} \quad (7)$$

$$Ag^+ + SO_4^{\bullet-} \leftrightarrow Ag^{2+} + SO_4^{2-} \quad (8)$$

$$Ag^+ + 2SO_4^{\bullet-} \leftrightarrow Ag^{3+} + SO_4^{2-} \quad (9)$$

$$Co^{2+} + SO_4^{\bullet-} \leftrightarrow Co^{3+} + SO_4^{2-} \quad (10)$$

3.2. Comparison with the Fenton Reagent

As mentioned before, hydroxyl radicals are very powerful oxidizing species that non-selectively attack and degrade organic compounds [24,37]. In our previous studies, we have used heterogeneous catalytic systems that generate $HO^{\bullet}$ to degrade MC-LR, and specifically, we utilized UVA* and solar light activated TiO_2-based photocatalysts [25–30]. FR is a homogeneous oxidizing system that generates free hydroxyl radicals. [16,18,31,64]. This was the first system which utilized transition metals, to catalyze the decomposition of oxidants (Eqs. (11)–(14)).

Our experiments were performed in the presence of atmospheric oxygen and *in-situ* generated O_2 from the reactions of all the systems (Eqs. (6) and (14)). Oxygen can act as an electron acceptor, propagate reactions and therefore enhance the degradation efficiencies [24]. Radiolabeled studies with O^{18} have shown that in the case of H_2O_2, the oxygen is formed from the same peroxide moiety, while in the case of PMS only the terminal oxygen from each HSO_5^- molecule is incorporated into the final O_2 product as shown in Eq. (6) [62]. Because of the iron speciation and precipitation at oxygenic environments at neutral pH, FR is usually applied at acidic conditions, unless a chelating agent is used [44,64].

$$Fe^{2+} + H_2O_2 \rightarrow Fe^{3+} + HO^{\bullet} + OH^- \quad (11)$$

$$Fe^{3+} + H_2O_2 \rightarrow Fe^{2+} + HO_2^{\bullet} + H^+ \quad (12)$$

$$Fe^{2+} + HO^{\bullet} \rightarrow Fe^{3+} + OH^- \quad (13)$$

$$Fe^{3+} + HO_2^{\bullet} \rightarrow Fe^{2+} + O_2 + H^+ \quad (14)$$

It was observed that hydrogen peroxide was not activated in the absence of Fe^{2+} and the concentration of MC-LR remained the same for the duration of the experiment (see Fig. 4 for controls). Control experiments on the possible hydrolysis of MC-LR at acidic conditions (pH 3.0) were also performed and no degradation of MC-LR occurred under these conditions either [30]. In the presence of

iron, the degradation of MC-LR was immediate and after 60 min of treatment, approximately 65% of the toxin was removed (Fig. 3). When the degradation was continued for another 3 h, a plateau was reached at $t = 2$ h and the degradation efficiency remained constant at ~80% (Fig. 4). These kinetics are very common for FR, irrespective of the contaminant used [16] and it is attributed to the requirement of high catalyst concentration for the decomposition of H_2O_2 to be initiated. This leads to the fast consumption of catalyst and high radical generation that rapidly react with the contaminant. Since the regeneration of the catalyst ($Fe^{3+} \rightarrow Fe^{2+}$, Eq. (12)) is not thermodynamically favorable ($E = -0.724$ V) [16], the FR system reaches a plateau and no further significant degradation is observed. This is a disadvantage of FR and FR-like systems because it has a limited role as a residual disinfectant and oxidant especially in soil remediation where the oxidant needs to be transported for long distances to reach the contaminant [19,20,45].

As shown in Fig. 3, coupling of PMS with a transition metal was the most successful system following the order $Co^{2+}/PMS > Fe^{2+}/H_2O_2 \gg Ag^{+}/PS$. In general, the oxidizing properties of peroxide oxidants are measured by the transfer of an e^- to a lower unoccupied molecular orbital (LUMO) [65]. Based on the LUMO properties of the oxidants their energy follows the order $H_2SO_5 < H_2O_2 < H_2S_2O_8$ [65], which means, that PMS accepts e^- more easily than the other oxidants. The ability of PMS to accept e^- is also demonstrated in the large number of transition metals (Ce^{3+}, Ru^{3+}, Fe^{2+}, Ti^{3+}, Mn^{2+}, Cu^{2+}) that can activate it, compared to other oxidants [17,38,60,66]. Moreover, Rastogi et al. [45] reported enhanced activation of PMS than that of PS with Fe^{2+} for the degradation of PCBs, which again can be attributed to the lower energy of the LUMO [65].

A comparison between FR to degrade MC-LR at its optimum treatment pH 3.0, and Co^{2+}/PMS at pH 3 and pH_{MQ} was conducted (Fig. 3). At pH 3.0, Co^{2+}/PMS system was not efficient and only 27% of MC-LR degraded after $t = 1$ h (Fig. 3). This reduction may be attributed to the inhibition of PMS to decompose at acidic pH, or the reaction of the sulfate radicals with the toxin. The rate of reaction between the formed radicals and the target contaminants is affected (i) by the rate of collision between the two, (ii) by the pH (i.e., $HO^\bullet + e^- + H^+ \rightarrow H_2O$, $E = 2.72$ V; $HO^\bullet + e^- \rightarrow HO^-$, $E = 1.99$ V) [37], (iii) the structure of the contaminant [16] and (iv) its overall charge [61]. In this study, the experiments were performed at pH values between $3 < pH < 6.4$, the overall charge of the toxin is singly negative for this pH range [30] and PMS was in ionized form (HSO_5^-, $pK_{a1} < 0$ and $pK_{a2} = 9.4$) [49]. As it will be discussed in an upcoming section (Section 3.3), the degradation of MC-LR by sulfate radicals was enhanced at acidic pH, however for the Co^{2+}/PMS/pH 3 system, the toxin concentration was not changed and only after the first hour a slight reduction in the toxin concentration was observed. Francis et al. have studied the decomposition of Co^{2+}/PMS at different pH values (pH 2, 5, 8) and found it to follow second order kinetics ($d[HSO_5^-]/dt = -k[HSO_5^-]^2$) [49]. At acidic pH, the decomposition of PMS was significantly decreased, drastically increased at pH 5 and then reduced again a pH 8 ($k_{pH2} = 0.003\ M^{-1}\ s^{-1}$, $k_{pH5} = 0.840\ M^{-1}\ s^{-1}$, $k_{pH8} = 0.105\ M^{-1}\ s^{-1}$) [49]. The authors reported that the decrease in the decomposition of PMS at basic conditions is due to the formation of hydroxides and hydrous oxides from the transition metals that changes the activation mechanisms of the oxidant. For acidic conditions, the sulfate radical anion has been reported to be involved in most of the free radical mechanisms that lead to PMS decomposition via e^- transfer [59]. Many researchers [17,49,62] seem to agree on the following mechanism for the Co^{2+} catalyzed decomposition of PMS:

$$Co^{2+} + HOOSO_3^- \leftrightarrow CoSO_5 + H^+ \quad (15)$$

$$CoSO_5 \rightarrow CoO^+ + SO_4^{\bullet -} \quad (16)$$

$$CoO^+ + 2H^+ \rightarrow Co^{3+} + H_2O \quad (17)$$

$$Co^{3+} + HOOSO_3^- \rightarrow Co^{2+} + {}^\bullet OOSO_3^- + H^+ \quad (2)$$

If the sulfate radicals are important in the propagation of PMS decomposition, then the increased acidity will prohibit the reaction (Eq. (15)) to occur, eventually resulting in slower degradation rates of the toxin.

3.3. Activation of oxidants with radiation

The activation of oxidants with UV radiation results in the homolytic cleavage of the peroxide bond and the formation of $SO_4^{\bullet -}$ and $HO^\bullet$ depending on the chemical structure of the oxidant (Eqs. (18)–(20)) [15,18–20]. Since hydrogen peroxide and persulfate are symmetric oxidants with respect to the peroxide bond, activation with UV radiation results in the formation of two hydroxyl or sulfate radicals, respectively (Eqs. (19) and (20)). On the other hand, PMS is asymmetric around the peroxide bond and cleaves to one $SO_4^{\bullet -}$ and one $HO^\bullet$ (Eq. (18)). Because during the photolysis of the oxidants, one type of radical is selectively formed, the results from these experiments could indicate the type of radical that is more reactive towards the oxidation of MC-LR.

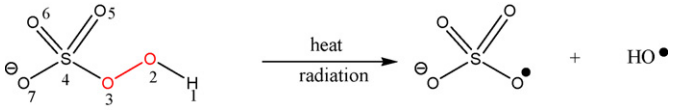

(18)

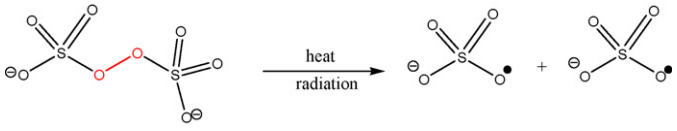

(19)

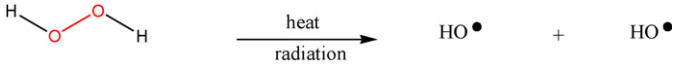

(20)

Many different types of radiation (including UV radiation, γ-radiation, pulse radiolysis) have been utilized to generate sulfate radicals by irradiating crystal powders of oxidant salts [67], aqueous solutions of PS and PMS [18,46,52,68,69], sulfite ions solutions [40], and concentrated sulfuric acid solutions [61,70,71]. Usually UVC ($\lambda = 254$ nm) radiation is utilized for the photolytic decomposition of oxidants [18] because of its high energy and high absorptivity of the oxidants at $\lambda = 254$ nm that can cause vibrations to the peroxide bond and eventually breaks it. However, in this study we chose to use UV ($300 < \lambda < 400$ nm) radiation for the activation of the oxidants to investigate whether a lower energy light source would successfully decompose the oxidants and efficiently degrade MC-LR. The maximum adsorption of MC-LR in the UV–vis spectra is observed at $\lambda = 238$ nm and UVA* radiation cannot cause it to lyse, while UVC radiation has been reported to cause isomerization of the diene bonds [29,72]. So any observed degradation with the Ox/UVA* system is most likely attributed to the free radicals.

The photolytic degradation of MC-LR at initial concentration 1000 μg/L (approximately equal to 1 μM of MC-LR) with molar ratios of oxidant to MC-LR between $5 < [Ox/MC\text{-}LR] < 100$ is shown in Figs. 4–6 and some of the controls (dark activation) in Fig. 4. The experiments were performed in MQ-H_2O in the absence of

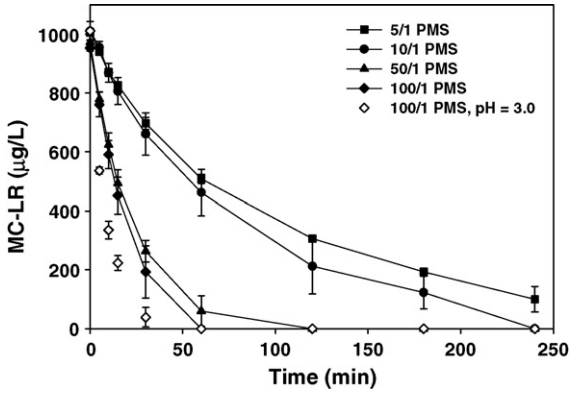

Fig. 5. Degradation of MC-LR with the PMS/UV (300 < λ < 400 nm) system at neutral pH at different PMS concentrations [$C_{MC\text{-}LR}$ = 1.0 μM; [PMS]/[MC-LR] molar ratio = 5–100].

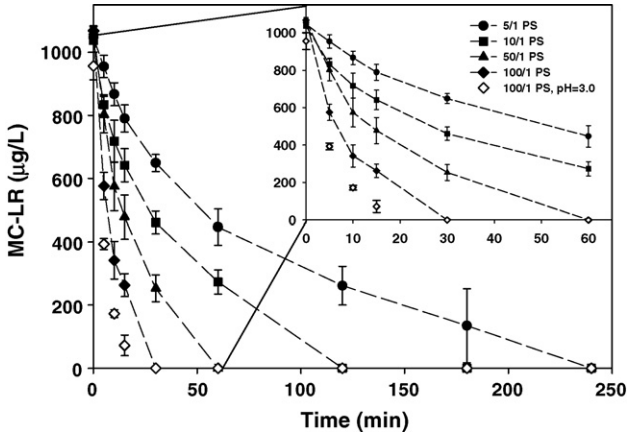

Fig. 6. Degradation of MC-LR with the PS/UV (300 < λ < 400 nm) system at neutral pH at different PS concentrations. Inner graph details the MC-LR concentration profiles from times 0 to 60 min [$C_{MC\text{-}LR}$ = 1.0 μM; [PMS]/[MC-LR] molar ratio = 5–100].

buffering solution (pH_{MQ} 5.8). In the case of PMS, increasing concentrations of oxidants caused a drop in pH (see Tables 1 and 2) because of the dissociation of HSO_4^- present in the OXONE® salt [45]. Starting with the activation of PMS in the dark, it was observed that at [PMS]/[MC-LR] = 5 and 10, no degradation of MC-LR occurred but for 50 and 100 ratios, approximately 50% of the toxin was removed after 4 h of contact time. This suggests that PMS is unstable and in aqueous solutions spontaneously decomposes even when kept in amber bottles. This is the reason why all the oxidant solutions used in this study were always freshly prepared [44,45]. Once UVA* radiation was applied, MC-LR removals greater than 90% were observed for all the [PMS]/[MC-LR] ratios at the end of treatment (Fig. 5). Based on the trends of the data, the disappearance of MC-LR was fitted with the *pseudo-first order* kinetic model (not shown here). Table 1 lists the initial rates of degradation (averaged at 15 min), the *first order* reaction kinetic constant, and the correlation coefficient (R^2) of the linear regression model. As in dark activation, the UVA* degradation of MC-LR for [PMS]/[MC-LR] = 5 and 10, and [PMS]/[MC-LR] = 50 and 100 followed similar trends and degradation efficiencies. The initial rates of the two pairs statistically analyzed using *t-test* (confidence level 95%) were found not to be different which suggests that for the PMS/UVA* system to increase its efficiency, the concentration of the oxidant needs to be increased by an order of magnitude. When the PMS/UVA* system was applied at acidic conditions (pH 3.0, [PMS]/[MC-LR] = 100) the initial rate of degradation and kinetic constant doubled compared to pH_{MQ}. This comes in contrast to the Co^{2+}/PMS/pH 3.0 system where low degradation rates were observed and verifies that reactivity of sulfate radicals under these conditions is not responsible for the low rates. In addition, it has been reported that the redox potential of the hydroxyl radicals (formed from the homolytic dissociation of PMS) increases at acidic conditions [37] and so does their reactivity.

Dark and UVA* activation of PS was performed under similar experimental conditions (Fig. 6). During dark activation, no degradation of MC-LR was observed for the lower [PS]/[MC-LR] molar ratios but approximately 25% of MC-LR was removed after 4 h with [PS]/[MC-LR] = 50 and 100. When UVA* radiation was used, the toxin was completely degraded by the end of treatment (t = 4 h). For the PS/UVA* system the degradation efficiency increased linearly with increasing oxidant concentration. The same trend is followed by the initial rates of degradation and the *pseudo-first order* kinetic constants (Table 2). At acidic conditions and molar ratio [PS]/[MC-LR] = 100, the system showed faster kinetics (k constant almost doubled) even though the initial rates of degradation between pH 3 and pH_{MQ} were not found to be statistically different. This reinforces that the efficiency of the sulfate radicals to oxidize organic

Table 1
Initial rates of degradation with increasing PMS concentration ($C_{MC\text{-}LR}$ = 1.0 μM).

[PMS/MC-LR] Molar ratio	Initial rates (nM/min)[a]	$k \times 10^3$ (min^{-1})	R^2	pH	$t_{EE/O}$ (min)	EE/O (kWh/m^3)
5	13.57 ± 5.49	9.98 ± 4.38	0.9955	6.24	240	7272
10	14.21 ± 4.00	13.22 ± 0.56	0.9968	6.24	190	5757
50	35.00 ± 3.36	44.54 ± 0.46	0.9999	5.87	55	1667
100	36.42 ± 1.35	52.02 ± 2.13	0.9976	4.81	45	1364
100	67.92 ± 1.92	110.02 ± 4.32	0.9971	3.00[b]	25	758

[a] Measured at t = 15 min.
[b] pH adjusted with H_2SO_4.

Table 2
Initial rates of degradation with increasing PS concentration ($C_{MC\text{-}LR}$ = 1.0 μM).

[PS/MC-LR] Molar ratio	Initial rates (nM/min)[a]	$k \times 10^3$ (min^{-1})	R^2	pH	$t_{EE/O}$ (min)	EE/O (kWh/m^3)
5	18.03 ± 4.61	13.00 ± 0.95	0.9907	6.11	195	5909
10	32.13 ± 6.14	25.78 ± 2.31	0.9899	6.03	100	3030
50	50.58 ± 4.51	53.93 ± 2.93	0.9957	6.33	50	1515
100	74.74 ± 5.53	109.90 ± 6.26	0.9940	6.39	25	758
100	78.72 ± 5.36	174.30 ± 1.51	0.9999	3.00[b]	15	455

[a] Measured at t = 15 min.
[b] pH adjusted with H_2SO_4.

compounds is not impaired at mild acidic conditions. In general, the PS/UVA* system gave better degradation efficiencies compared to the PMS/UVA* at all tested ratios.

Finally, the PMS/UVA* and PS/UVA* systems were compared with the H_2O_2/UVA* (Fig. 4). H_2O_2 was the most stable oxidant in aqueous solution and no degradation of MC-LR was observed during dark adsorption even at [H_2O_2]/[MC-LR] = 100 which may be due to H_2O_2 peroxide solution preparation by diluting aliquots of the stabilized peroxide standard solution (ACROS) into MQ-H_2O. When UVA* radiation was applied, the toxin degraded gradually and was completely removed by the end of the 4 h treatment. The UVA*/H_2O_2 degradation data were also fitted with the *first order* kinetic model ($R^2 = 0.9979$) with $k = (10.06 \pm 0.31) \times 10^{-3}$ min^{-1}. Compared with PMS/UVA* and PS/UVA,* the H_2O_2/UVA* was significantly slower by at least one order of magnitude based on the k constants.

Besides kinetics, a more comprehensive way to compare the effectiveness of UV-based technologies has been adopted by the Photochemistry Commission of International Union of Pure chemistry, the *electrical energy per order* (*EE/O*) [15,18]. *EE/O* measures the electrical energy (kWh) that is required to reduce the concentration of a contaminant by an order of magnitude in a 1 m^3 (1000 L) solution or air, and is described by the following equation:

$$EE/O = \frac{Pt}{60V}\left(\frac{kW}{m^3} = \frac{W}{L}\right) \quad (21)$$

where *EE/O*, electrical energy per order; *P*, total electrical power or flux entering the reactor (W); *t*, time (min); *V*, volume of water treated (L).

The times where the contaminant was reduced by an order of magnitude were estimated from the graphs in Figs. 4–6 by finding the time that corresponds to remaining toxin concentration equal to 100 μg/L. The *EE/O* values along with the times are listed in Tables 1 and 2, with the smallest *EE/O* value representing the more energy efficient technology. Overall, the Ox/UVA* activation followed the order of PS/UVA* > PMS/UVA* ≫ H_2O_2/UVA* independently of the solution pH and oxidant concentration. At acidic pH 3.0, the PS/UVA* system with molar ratio [PS]/[MC-LR] = 100 was the most efficient under the conditions tested in this study.

3.4. Activation of oxidants with heat

Thermal activation of the oxidants results in their homolytic decomposition as described in the previous section. This technology has been applied in soil remediation [20] and for the treatment of chlorinated ethenes [19]. The oxidants were activated at $T = 30$ °C (lowest temperature that has been used in the literature, [19] and at specific time intervals the corresponding UV–vis spectra were taken (Figs. 7–9). The UV–vis spectra of the oxidants, MC-LR, as well as their combination were recorded at $T = 25$ °C, to account for any changes during the thermal activation (Figs. 9–11). The initial and final concentration of the toxin at each experiment was determined by HPLC analysis (Fig. 12). From the recorded spectra, it is apparent that there is no complexation reaction occurring between the toxin and the oxidant since we could not detect any newly formed peaks during treatment. The spectra of the solutions that contained the oxidant and toxin together appear to be the addition of the individual spectra for each component (Figs. 9–11). The depletion of the concentration of MC-LR was monitored by the reduction in the absorption at $\lambda = 238$ nm (MC-LR's maxima). For the PMS + MC-LR system, the peak rapidly reduced with time and at $t = 3.5$ h almost disappeared from the spectrum. The overall toxin removal with PMS was ~77%. For PS + MC-LR the reaction rate was slower and at the end of the treatment ~52% of the toxin was removed. For H_2O_2 the degradation was negligible (~3%) at $T = 30$ °C, so the temperature was increased to $T = 37$ °C for an additional $t = 15$ min and an additional 1% of degradation was achieved. Based on these observations, H_2O_2 requires higher temperatures to get activated and therefore the degradation efficiency order from the thermal activation of the oxidants is PMS > PS ≫ H_2O_2.

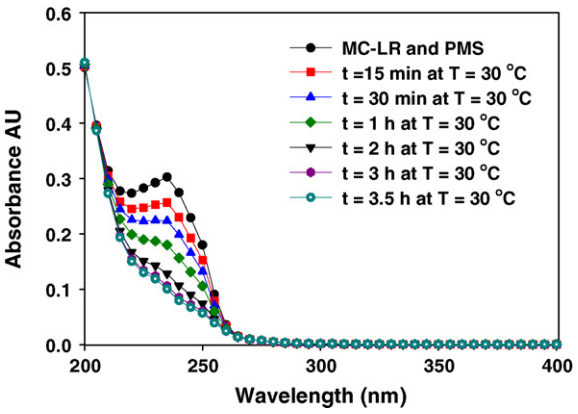

Fig. 7. UV–vis Spectra of the thermal degradation of MC-LR with PMS at $T = 30$ °C [$C_{MC-LR} = 10.0$ μM; [PMS]/[MC-LR] = 100, pH 4.81].

3.5. Comparison between oxidation systems during homolytic dissociation

The dissociation energies of the peroxide bonds as well as the bond length can provide useful information on the reactiv-

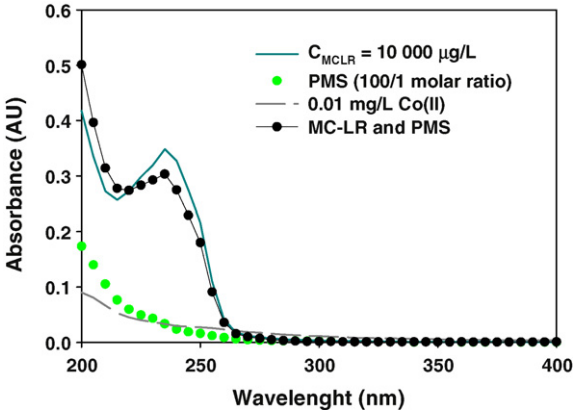

Fig. 8. UV–vis Spectra of the thermal degradation of MC-LR with PS at $T = 30$ °C [$C_{MC-LR} = 10.0$ μM; [PS]/[MC-LR] = 100, pH 6. 39].

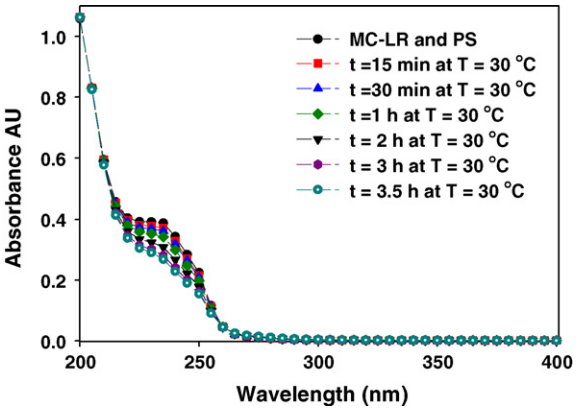

Fig. 9. UV–vis spectra of MC-LR alone, and H_2O_2 alone at $T = 25$ °C and during the thermal degradation of MC-LR with H_2O_2 at $T = 30$ °C [$C_{MC-LR} = 10.0$ μM; [H_2O_2]/[MC-LR] = 100].

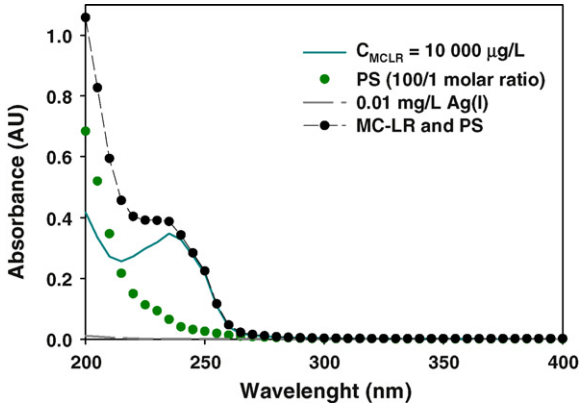

Fig. 10. UV–vis Spectra of MC-LR alone, Co(II) alone and PMS alone at $T = 25\,^{\circ}C$, and PMS + MC-LR at $T = 30\,^{\circ}C$ [Co(II) = 0.01 mg/L; $C_{MC\text{-}LR} = 10.0\,\mu M$; [PMS]/[MC-LR] = 100].

ity of the oxidants and possible explanations to our experimental results. In general, the reported dissociation energies of peroxide bonds (O–O) are much lower than the bond of oxygen with other atoms (i.e., $\Delta H_{C-O} = 84$ kcal/mol, $\Delta H_{F-O} = 44$ kcal/mol) [73]. The high reactivity of this group justifies the weakness of the O–O bond and its homolytic dissociation [73]. A generic enthalpy value of $\Delta H_{O-O} = 34$ kcal/mol was assigned for the cleavage of peroxide bonds [73]. However, studies have shown that the close environment (ligands) of the peroxide bond affects its dissociation energy [73]. For H_2O_2 and PMS the dissociation enthalpies of the peroxide bond were estimated to be 38–52 kcal/mol [65] (50 kcal/mol from [73]) and 33.5 kcal/mol [18,65], respectively. Since PMS is the combination of H_2O_2 and $S_2O_8^{2-}$, its dissociation energy could be derived from their mean $\Delta H_{O-O} = 41.75$ kcal/mol. This is a commonly used approach for calculating bond ΔH [73]. Another approach to assess the reactivity of an oxidant is the length of the peroxide bond [18]. The peroxide bond for all three oxidants is a σ-bond created from the same orbitals [65] with estimated lengths 1.453 Å for H_2O_2, 1.460 Å for H_2SO_5, $H_2S_2O_8$ [65] and $KHSO_5{\cdot}H_2O$ [74], while for the ammonium salt of PS is 1.497 Å [74]. Based on this information, the peroxide bond length for PS and PMS are quite close (if not the same) and therefore the decomposition order by homolytic cleavage should be PS ≥ PMS > H_2O_2. Meunier [75] hypothesized that the asymmetric structure of the peroxide bond of the PMS might make it to be more susceptible to cleavage . If this statement is true then it is in agreement with the order that we observed during thermolysis of the oxidants: PMS > PS ≫ H_2O_2.

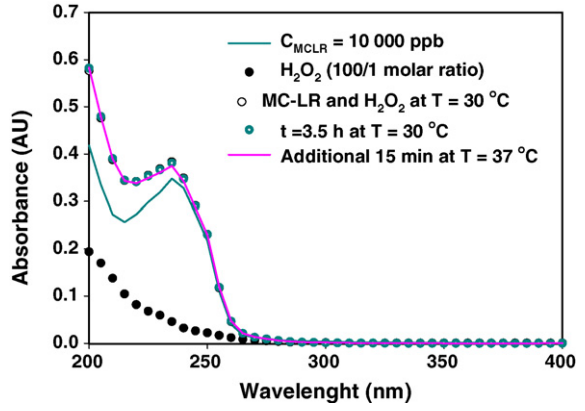

Fig. 11. UV–vis spectra of MC-LR alone, Ag(I) alone and PS alone at $T = 25\,^{\circ}C$, and PS + MC-LR at $T = 30\,^{\circ}C$ [Ag(I) = 0.01 mg/L; $C_{MC\text{-}LR} = 10.0\,\mu M$; [PMS]/[MC-LR] = 100].

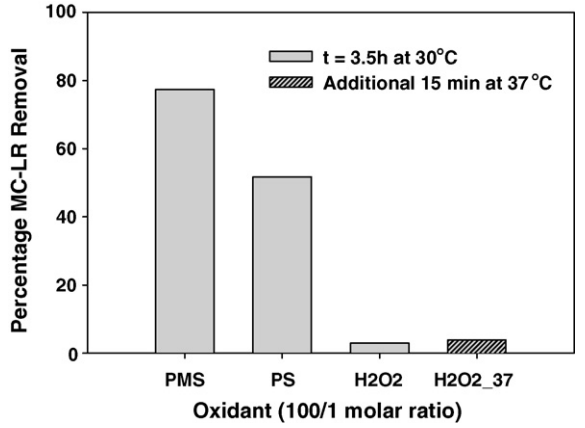

Fig. 12. Percentage of MC-LR removal after the thermal activation ($T = 30\,^{\circ}C$) of the oxidants PMS, PS and H_2O_2 for $t = 3.5$ h. For H_2O_2 additional 15 min at $T = 37\,^{\circ}C$ [$C_{MC\text{-}LR} = 10.0\,\mu M$; [Ox]/[MC-LR] = 100].

During the photolysis of the oxidants, the effectiveness of the systems followed the order PS > PMS ≫ H_2O_2 which complies with the estimated activation energies for each oxidant. Based on Anipsitakis and Dionysiou [18], besides the activation energy of a compound under UV radiation its ability to absorb the available energy is also very important. For this reason, the UV–vis spectra of the toxin and oxidants (alone and in pairs) at $T = 25\,^{\circ}C$ were recorded. The maximum absorption occurs between $200 < \lambda < 250$ nm while for the remaining wavelengths were weak, possibly because of the low oxidants concentrations (μM) used in this study. At higher oxidants concentrations, (>mM) the absorption values increased and for $\lambda > 300$ nm were in the same range as for UVC activation ($\lambda = 254$ nm) [18]. We strongly believe that the activation of the oxidants does not come from absorbing radiation only at the $\lambda_{max} = 365$ nm, but from the whole emission spectra of the lamps ($300 < \lambda < 400$ nm). In addition, Atkins et al. [67] have reported that irradiated crystals of PS at $\lambda = 365$ nm caused the formation of $SO_4^{\bullet -}$. Finally, a study has shown that the extinction coefficient of these oxidants follows the order PS > PMS > H_2O_2 through out the UV–vis spectra [18], which complies with the activation order established in this study.

4. Conclusion

This study investigated different advanced oxidation systems that produce sulfate radicals for the destruction of a naturally occurring toxin in water resources, the hepatotoxin MC-LR. The efficiencies of these systems were also compared with their corresponding hydroxyl radical-based systems. Specifically, the oxidant peroxymonosulfate (PMS), persulfate (PS) and hydrogen peroxide (H_2O_2) were activated with catalysts (M^{n+}/Ox), radiation (Ox/UVA*) or heat (Ox/$T = 30\,^{\circ}C$). Based on the chemical structures of PS and PMS, they are the salt derivatives of modified hydrogen peroxide from inorganic salts which is indicative of the similarities, and differences of these oxidants [65]. When the decomposition of the oxidants was catalyzed by transition metals, the order Co^{2+}/PMS > Fe^{2+}/H_2O_2 ≫ Ag^+/PS, was observed with respect to their MC-LR degradation efficiencies at the optimum pH values for each system. When the oxidants were irradiated with UVA* lamps, the efficiency decreased from PS > PMS ≫ H_2O_2 and enhanced at acidic pH in the same order. During the thermolysis of the oxidants, PMS was the most efficient followed by PS, while H_2O_2 required higher temperatures. Our results are compatible with the energies of the LUMO as well as length and strength of the peroxide bond for each oxidant. This study has shown that sulfate radical-based AOTs are capable at degrading complex and unconventional contaminants such as the cyanotoxins at comparable and higher rates than certain hydroxyl radical-based AOTs.

Acknowledgments

This research was funded in part by the National Science Foundation through a CAREER Award (BES-0448117) to D.D.D., the U.S. EPA (RD-83322301) and the Center of Sustainable Urban Engineering (SUE) at the University of Cincinnati (UC). M.G.A. is grateful to *Sigma Xi*, The Scientific Society for a Grant-in-Aid of Research Fellowship, the Rindsberg Memorial Fund of UC and the University Research Council of UC for a Graduate School Distinguished Dissertation Completion Fellowship. M.G.A. is also thankful to Dr. Shirish Agarwal (UC) and Dr. George P. Anipsitakis for their insightful input.

Disclaimer

Although this work was reviewed by US EPA and approved for publication, it may not necessarily reflect official Agency policy.

References

[1] M.G. Antoniou, A.A. de la Cruz, D.D. Dionysiou, Journal of Environmental Engineering 131 (2005) 1239–1243.
[2] China Vows to Clean Up Polluted Lake, Retrieved November 9, 2009, http://www.nytimes.com/2007/10/27/world/asia/27china.html?scp=2&sq=Lake+tai&st=nyt.
[3] G. Newcombe, M. Burch, Opflow, vol. 29, American Water Works Association, 2003, pp. 1239–1243.
[4] W.W. Carmichael, Journal of Applied Bacteriology 72 (1992) 445–459.
[5] W.W. Carmichael, S.M.F.O. Azevedo, J.S. An, R.J.R. Molica, E.M. Jochimsen, S. Lau, K.L. Rinehart, G.R. Shaw, G.K. Eaglesham, Environmental Health Perspectives 109 (2001) 663–668.
[6] S.M.F.O. Azevedo, W.W. Carmichael, E.M. Jochimsen, K.L. Rinehart, S. Lau, G.R. Shaw, G.K. Eaglesham, Toxicology 181–182 (2002) 441–446.
[7] E.D. Hilborn, W.W. Carmichael, R.M. Soares, M. Yuan, J.C. Servaites, H.A. Barton, S.M.F.O. Azevedo, Environmental Toxicology 22 (2007) 459–463.
[8] C.W. Diehnelt, S.M. Peterman, W.L. Budde, TrAC – Trends in Analytical Chemistry 24 (2005) 622–634.
[9] H. Konst, P.D. McKercher, P.R. Gorham, A. Robertson, J. Howell, Canadian Journal of Comparative Medicine and Veterinary Science 29 (1965) 221–228.
[10] C. Wiegand, S. Pflugmacher, Toxicology and Applied Pharmacology 203 (2005) 201–218.
[11] L.A. Lawton, P.K.J. Robertson, Chemical Society Reviews 28 (1999) 217–224.
[12] K. Tsuji, T. Watanuki, F. Kondo, M.F. Watanabe, S. Suzuki, H. Nakazawa, M. Suzuki, H. Uchida, K. Harada, Toxicon 33 (1995) 1619–1631.
[13] K. Harada, K. Tsuji, Journal of Toxicology – Toxin Reviews 17 (1998) 385–403.
[14] S.D. Richardson, Analytical Chemistry 81 (2009) 4645–4677.
[15] J.R. Bolton, Ultraviolet Applications Handbook, 2nd ed., Bolton Photosciences Inc., 2001, pp. 27.
[16] G.P. Anipsitakis, D.D. Dionysiou, Environmental Science and Technology 37 (2003) 4790–4797.
[17] G.P. Anipsitakis, D.D. Dionysiou, Environmental Science and Technology 38 (2004) 3705–3712.
[18] G.P. Anipsitakis, D.D. Dionysiou, Applied Catalysis B: Environmental 54 (2004) 155–163.
[19] R.H. Waldemer, P.G. Tratnyek, R.L. Johnson, J.T. Nurmi, Environmental Science and Technology 41 (2007) 1010–1015.
[20] R.L. Johnson, P.G. Tratnyek, R.O. Johnson, Environmental Science and Technology 42 (2008) 9350–9356.
[21] I. Balakrishnan, M.P. Reddy, Journal of Physical Chemistry 74 (1970) 850–855.
[22] W. Song, T. Teshiba, K. Rein, K.E. O'Shea, Environmental Science and Technology 39 (2005) 6300–6305.
[23] W. Song, A.A. De La Cruz, K. Rein, K.E. O'Shea, Environmental Science and Technology 40 (2006) 3941–3946.
[24] M.R. Hoffmann, S.T. Martin, W. Choi, D.W. Bahnemann, Chemical Reviews 95 (1995) 69–96.
[25] H. Choi, M.G. Antoniou, M. Pelaez, A.A. De La Cruz, J.A. Shoemaker, D.D. Dionysiou, Environmental Science and Technology 41 (2007) 7530–7535.
[26] H. Choi, M.G. Antoniou, A.A. de la Cruz, E. Stathatos, D.D. Dionysiou, Desalination 202 (2007) 199–206.
[27] M.G. Antoniou, D.D. Dionysiou, Catalysis Today 124 (2007) 215–223.
[28] M.G. Antoniou, J.A. Shoemaker, A.A. de la Cruz, D.D. Dionysiou, Toxicon 51 (2008) 1103–1118.
[29] M.G. Antoniou, J.A. Shoemaker, A.A. De La Cruz, D.D. Dionysiou, Environmental Science and Technology 42 (2008) 8877–8883.
[30] M.G. Antoniou, P.A. Nicolaou, J.A. Shoemaker, A.A. de la Cruz, D.D. Dionysiou, Applied Catalysis B: Environmental 91 (2009) 165–173.
[31] E.R. Bandala, D. Martiĩnez, E. Martiĩnez, D.D. Dionysiou, Toxicon 43 (2004) 829–832.
[32] G.P. Anipsitakis, E. Stathatos, D.D. Dionysiou, Journal of Physical Chemistry B 109 (2005) 13052–13055.
[33] G.P. Anipsitakis, D.D. Dionysiou, M.A. Gonzalez, Environmental Science and Technology 40 (2006) 1000–1007.
[34] G.P. Anipsitakis, T.P. Tufano, D.D. Dionysiou, Water Research 42 (2008) 2899–2910.
[35] L. Eberson, in: V. Gold, D. Bethell (Eds.), Advances in Physical Organic Chemistry, Academic Press, 1982, pp. 79–185.
[36] P. Neta, R.E. Huie, A.B. Ross, Journal of Physical and Chemical Reference Data 17 (1988) 1027–1284.
[37] G.V. Buxton, C.L. Greenstock, W.P. Helman, A.B. Ross, Journal of Physical and Chemical Reference Data 17 (1988) 513–886.
[38] J.E. Bennett, B.C. Gilbert, J.K. Stell, Journal of the Chemical Society, Perkin Transactions 2 (1991) 1105–1110.
[39] A.K. Pikaev, V.I. Zolotarevskii, Bulletin of the Academy of Sciences of the USSR Division of Chemical Science 16 (1967) 181–182.
[40] E. Hayon, A. Treinin, J. Wilf, Journal of American Chemical Society 94 (1972) 47–57.
[41] S. You, Q. Zhao, J. Zhang, J. Jiang, S. Zhao, Journal of Power Sources 162 (2006) 1409–1415, doi:10.1016/j.jpowsour.2006.07.063.
[42] O Legrini, E. Oliveros, A.M. Braun, Chemical Reviews 93 (1993) 671–698.
[43] P. Neta, V. Madhavan, H. Zemel, R.W. Fessenden, Journal of the American Chemical Society 99 (1977) 163–164.
[44] A. Rastogi, S.R. Al-Abed, D.D. Dionysiou, Water Research 43 (2009) 684–694.
[45] A. Rastogi, S.R. Al-Abed, D.D. Dionysiou, Applied Catalysis B: Environmental 85 (2009) 171–179.
[46] Q. Yang, H. Choi, Y. Chen, D.D. Dionysiou, Applied Catalysis B: Environmental 77 (2008) 300–307.
[47] Q. Yang, H. Choi, D.D. Dionysiou, Applied Catalysis B: Environmental 74 (2007) 170–178.
[48] I.K. Konstantinou, T.A. Albanis, Applied Catalysis B: Environmental 49 (2004) 1–14, doi:10.1016/j.apcatb.2003.11.010.
[49] R.C. Francis, X. Zhang, P.M. Froass, O. Tamer, Tappi Journal 77 (1994) 133–140.
[50] A.R. Negri, G. Jiménez, R.T. Hill, R.C. Francis, Tappi Journal 81 (1998) 241–246.
[51] G.R. Peyton, Marine Chemistry 41 (1993) 91–103.
[52] G. Mark, M.N. Schuchmann, H.-. Schuchmann, C. von Sonntag, Journal of Photochemistry and Photobiology, A: Chemistry 55 (1990) 157–168.
[53] N. Nieto, I.J. Munslow, J. Barr, J. Benet-Buchholz, A. Vidal-Ferran, Organic and Biomolecular Chemistry 6 (2008) 2276–2281.
[54] UVA Spectra, Retrieved November 9, 2009, http://www.uvp.com/pdf/365.pdf.
[55] S.L. Murov, I. Carmichael, G.L. Hug, Handbook of Photochemistry, 2nd ed. (revised and expanded), Marcel Dekker, New York, 1993, pp. 298–305.
[56] S. Goldstein, J. Rabani, Journal of Photochemistry and Photobiology A 193 (2008) 50–55.
[57] K.K. Rohatgi-Mukherjee, Fundamentals of Photochemistry, New Age International, 1978.
[58] C. Brandt, R. Van Eldik, Chemical Reviews 95 (1995) 119–190.
[59] C. Marsh, J.O. Edwards, Progress in Reaction Kinetics 15 (1989) 35–75.
[60] B.C. Gilbert, J.K. Stell, Journal of the Chemical Society, Perkin Transactions 2 (1990) 1281–1288.
[61] D.G. Marketos, Zeitschrift fuer Physikalische Chemie (Muenchen, Germany) 65 (1969) 306–321.
[62] R.C. Thompson, Inorganic Chemistry 20 (1981) 1005–1010.
[63] D.A. House, Chemical Reviews 62 (1962) 185–203.
[64] P. Gajdek, Z. Lechowski, T. Bochnia, M. Kepczyniski, Toxicon 39 (2001) 1575–1578.
[65] A.G. Miroshnichenko, V.A. Lunenok-Burmakina, Theoretical and Experimental Chemistry 11 (1976) 320–325.
[66] B.C. Gilbert, J.K. Stell, Journal of the Chemical Society, Faraday Transactions 86 (1990) 3261–3266.
[67] P.W. Atkins, M.C.R. Symons, P.A. Trevalion, Proceedings of the Chemical Society, 1963, p. 222.
[68] M.-. Tsao, W.K. Wilmarth, Journal of Physical Chemistry 63 (1959) 346–353.
[69] I. Kraljić, International Journal for Radiation Physics and Chemistry 2 (1970) 59–68.
[70] G.G. Mihai, P.G. Tarassoff, N. Filipescu, Journal of the Chemical Society, Perkin Transactions 1 (1975) 1374–1376.
[71] P. Jiang, Y. Katsumura, M. Domae, K. Ishikawa, R. Nagaishi, K. Ishigure, Y. Yoshida, Journal of the Chemical Society, Faraday Transactions 88 (1992) 3319–3322.
[72] K.-I. Harada, K. Ogawa, K. Matsuura, H. Murata, M. Suzuki, M.F. Watanabe, Y. Itezono, N. Nakayama, Chemical Research in Toxicology 3 (1990) 473–481.
[73] R.D. Bach, P.Y. Ayala, H.B. Schlegel, Journal of American Chemical Society 118 (1996) 12758–12765.
[74] J. Flanagan, W.P. Griffith, A.C. Skapski, Journal of Chemical Society, Chemical Communication (1984) 1574–1575.
[75] B. Meunier, New Journal of Chemistry 16 (1992) 203–211.